Supporting Information:

Fragile protein folds: Sequence and environmental factors affecting the equilibrium of two interconverting, stably folded protein conformations

Xingjian Xu[1,2], Igor Dikiy[1,3], Matthew Evans[4], Leandro P. Marcelino[1,5], Kevin H. Gardner[1,5,6]

[1]Structural Biology Initiative, CUNY Advanced Science Research Center, New York, NY, USA

[2]Ph.D Program in Biochemistry, The Graduate Center, CUNY, New York, NY, USA

[3]Current address: Regeneron Pharmaceuticals, Tarrytown, NY, USA

[4]Current affiliation: Acclaim Physician Group, Inc. Fort Worth, Texas, USA

[5]Department of Chemistry and Biochemistry, City College of New York, New York, NY, USA

[6]Biochemistry, Chemistry and Biology PhD Programs, Graduate Center, The City University of New York, New York, NY, USA

Correspondence: Kevin Gardner (kgardner@gc.cuny.edu)

Supplementary Figures

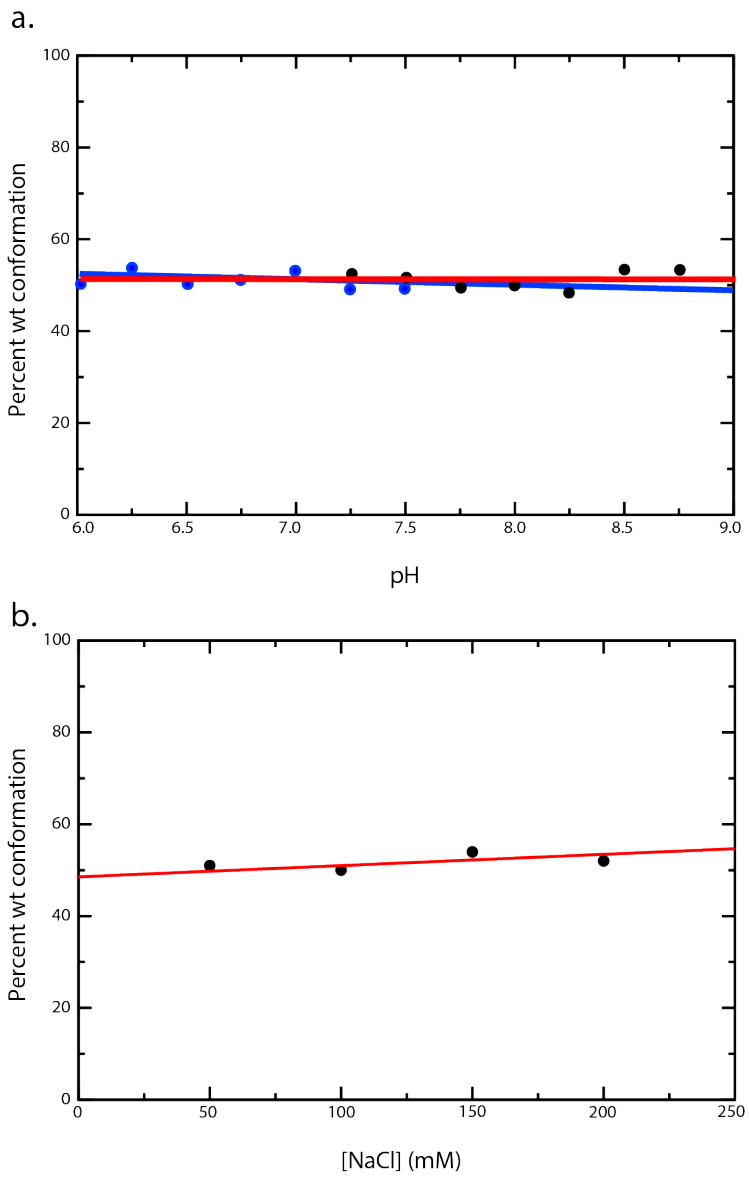

Supplementary Figure S1 – pH and salt concentration have negligible effects on WT :SLIP equilibrium. (a) The equilibrium remains the same throughout a pH titration between pH 7.0 and 9.0 in Tris (black circles, red line) or between pH 6.0 and 7.5 in PIPES (blue circles, blue line), with XX mM NaCl present at all points. The lines represent linear regressions to the data points. (b) The equilibrium remains mostly the same throughout a NaCl titration between 50 and 200 mM (black circles, red line), all at pH XX. The line represents a linear regression to the data points.

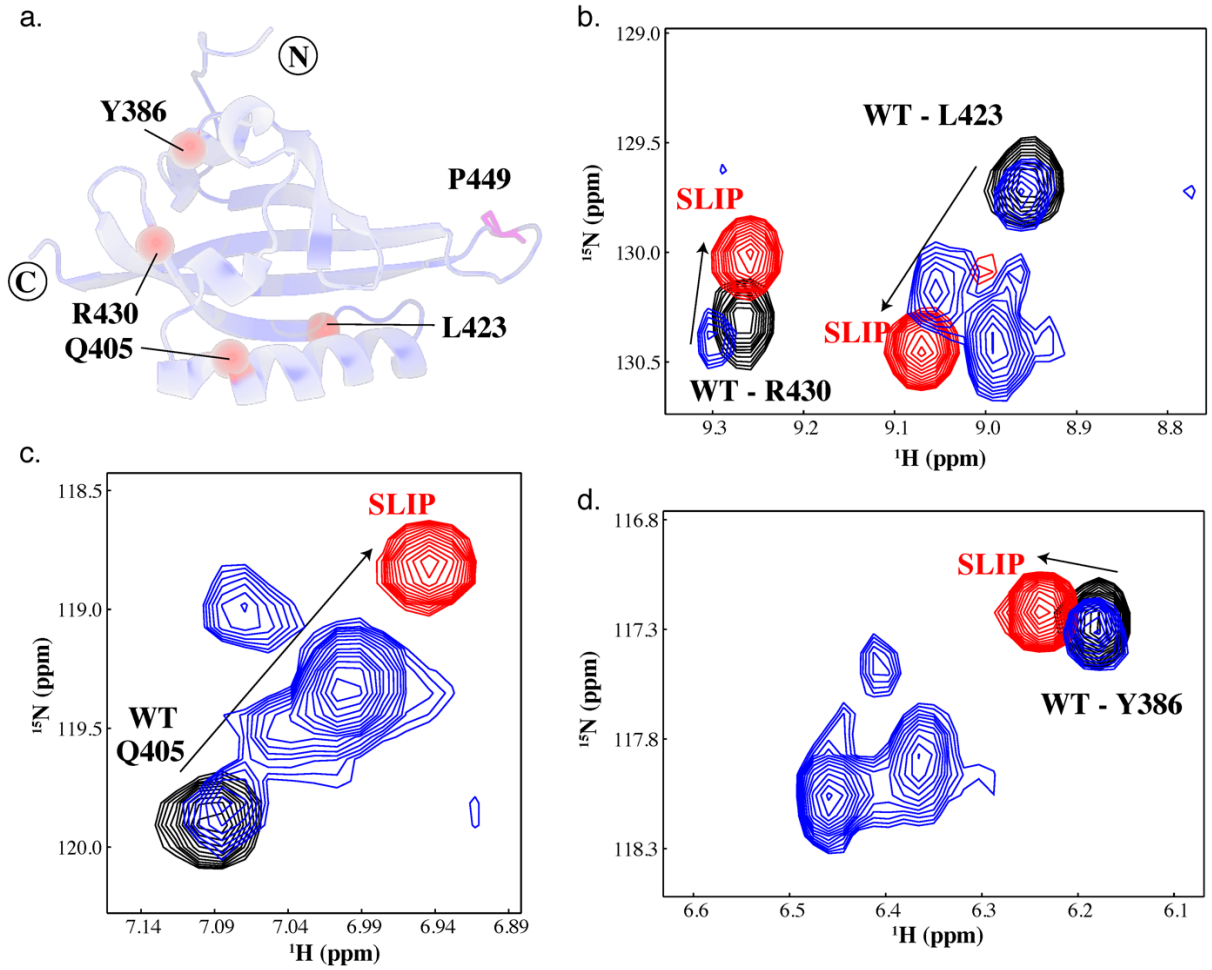

Supplementary Figure S2 – Mutations at position P449 produce multiple conformations of ARNT PAS-B. (a) A schematic of the solution structure of wildtype ARNT PAS-B domain (PDB code: 1X0O, (Card et al., 2005)). Substitution of alanine for proline at position 449, displayed in magenta sticks, causes global conformational changes. (b-d) Widespread peak doubling is observed throughout ^{15}N-^{1}H HSQC spectra as probed at residues Y386, Q405, L423, and R340. Proteins: wildtype (black), F444Q/F446A/Y456T (red) and P449A (blue).

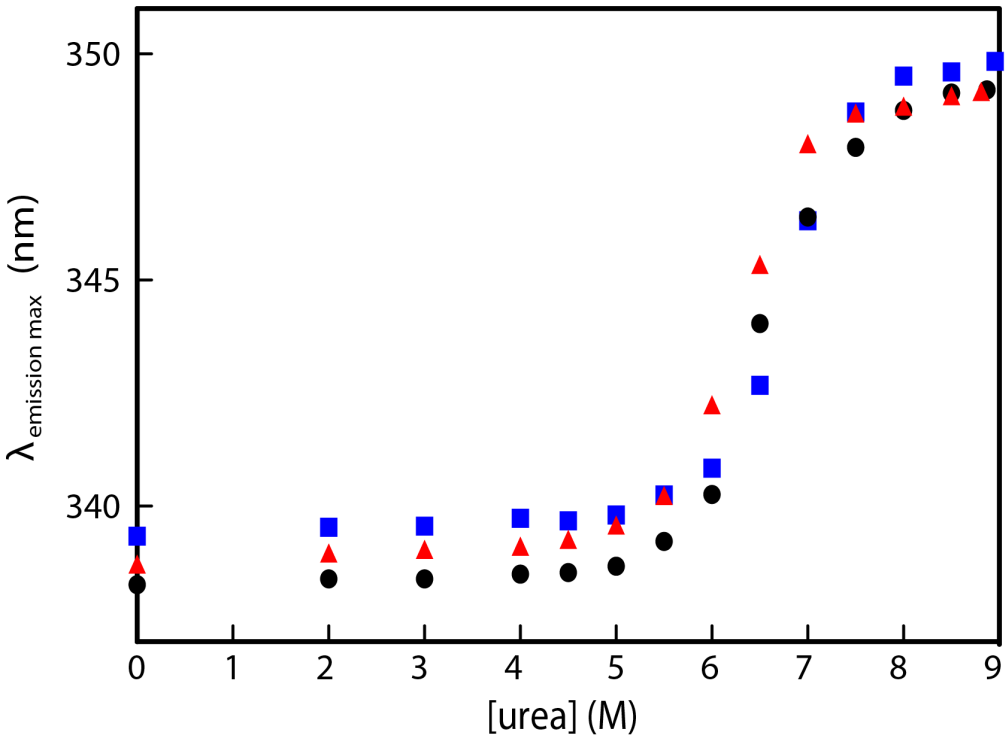

Supplementary Figure S3 – ARNT PAS-B variants have similar urea denaturation curves. The peak emission wavelength of ARNT PAS-B wildtype (black circles), Y456T (red triangles), and F444A/F446Q/Y456T (blue squares) red shifted with increasing concentrations of urea as the proteins unfolded. The mutants are roughly as stable as the wildtype protein.

a

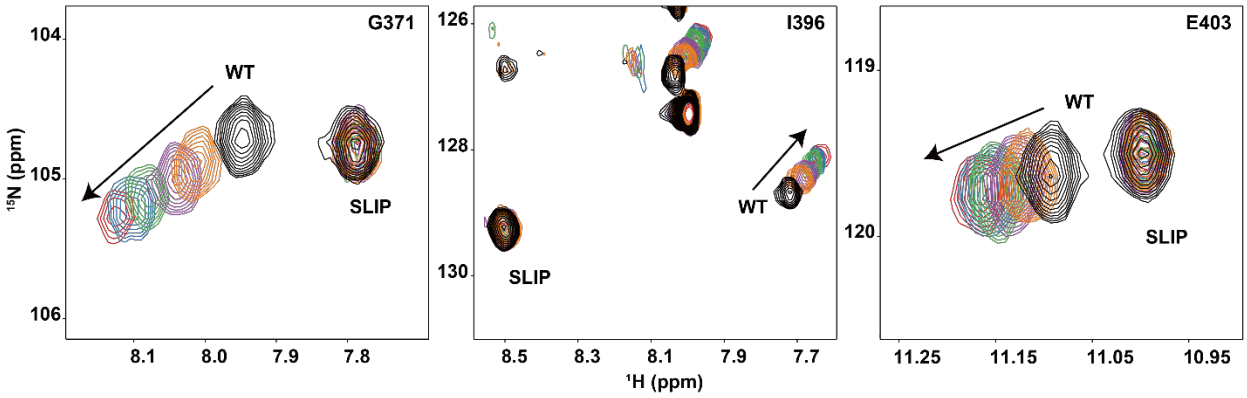
G371
I396
E403
WT
SLIP
WT
SLIP
WT
SLIP
^{15}N (ppm)
^{1}H (ppm)

b

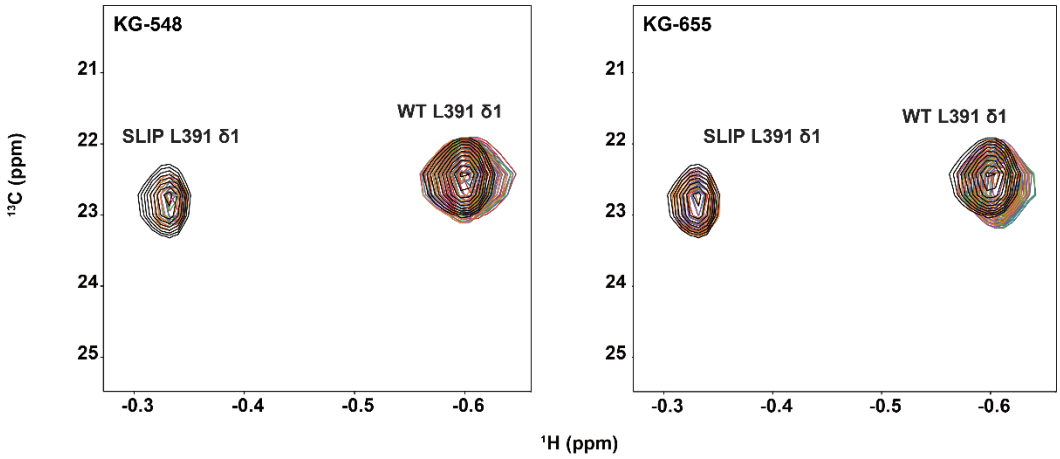
KG-548
KG-655
SLIP L391 δ1
WT L391 δ1
SLIP L391 δ1
WT L391 δ1
^{13}C (ppm)
^{1}H (ppm)

c

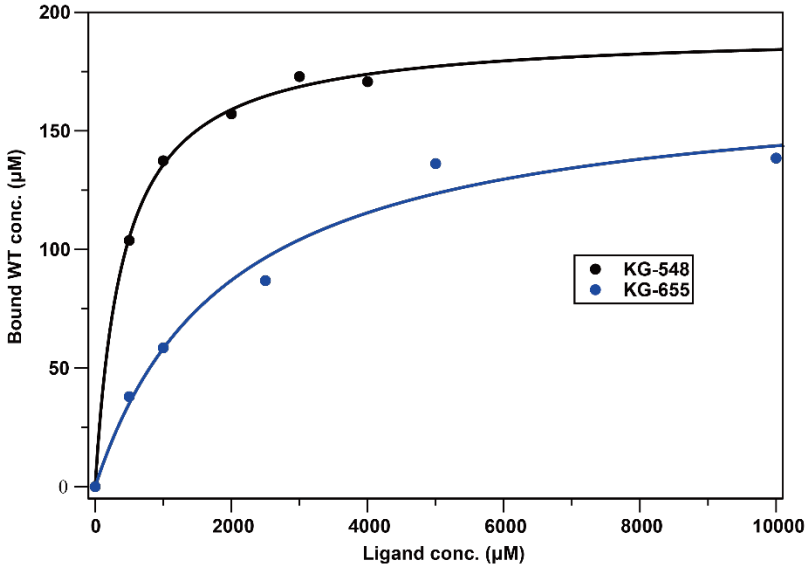
KG-548
KG-655
Bound WT conc. (μM)
Ligand conc. (μM)

Supplementary Figure S4 – KG-548 and KG-655 binding titration analysis using ^{13}C-^{1}H HSQC. (a) Example peaks from ^{15}N-^{1}H HSQC spectra of KG-655 titration series (0, 500, 1000, 2500, 5000, 10000 μM) against 250 μM ARNT PAS-B Y456T. Peaks associated with the WT conformation show chemical shift changes, while peaks associated with the SLIP conformation do not, suggesting selective binding. Unlike KG-548, many analyzable residues (where both WT and SLIP peaks are assigned) are directly involved with ligand binding and showing mixed fast-intermediate exchange characteristics in NMR spectra. (b) ^{13}C-^{1}H HSQC titration experiments of KG-548 (0, 500, 1000, 2000, 3000, 4000 μM) and KG-655 (0, 500, 1000, 2500, 5000, 10000 μM) against 250 μM ARNT PAS-B Y456T, focusing on the L391 δ1 methyl signals. Both WT and SLIP peaks are well resolved at all compound concentrations with no sign of peak broadening. Chemical shift changes to the WT conformation are minimal in the presence of both KG-548 and KG-655, suggesting the residue is not directly involved in the binding of either compounds. (c) KG-548 and KG-655 binding to ARNT PAS-B Y456T as monitored by peak volumes of L391 δ1 from ^{13}C-^{1}H HSQC NMR spectra. Data are fit to Eq. 1 to extract dissociation constant K_d and maximum binding B_{max}; resulting values are K_d = 414 ± 7.1 μM and B_{max} = 192 ± 0.96 μM for KG-548, and K_d = 1947 ± 152 μM and B_{max} = 172 ± 5.7 μM for KG-655. Uncertainties were estimated using bootstrapping. Noises with mean of 0 and variance of the standard error were added to the experimental data. Generated datasets (n = 30) were fit to obtain the 95% confidence interval.

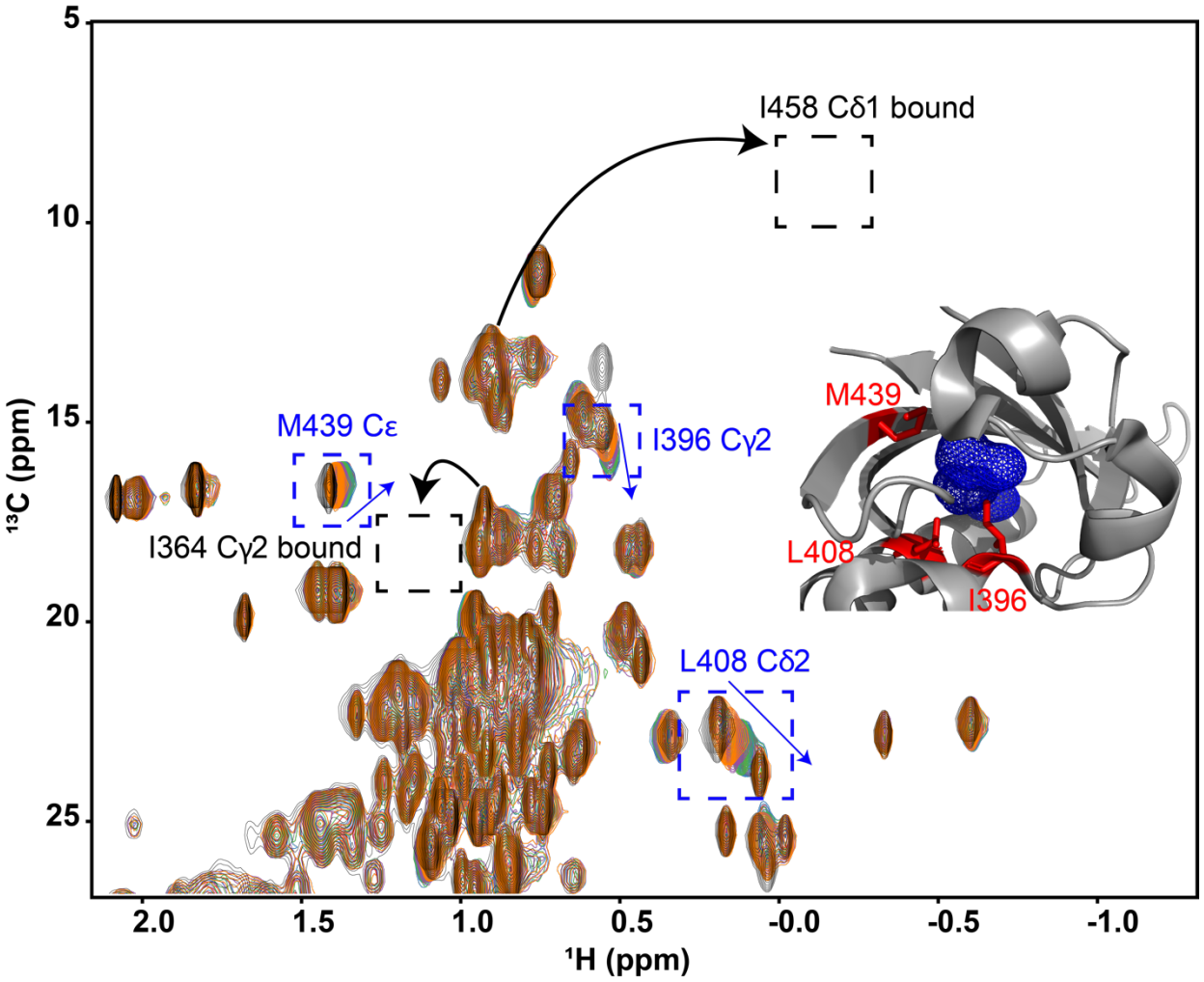

Supplementary Figure S5 – KG-655 loses surface binding to the WT conformation of ARNT PAS-B Y456T while retaining the internal binding mode. Shown here is the ^{13}C-^{1}H HSQC titration series of KG-655 (0 – 10 mM) against ARNT PAS-B Y456T, zoomed in on the methyl region. As previously reported, KG-655 binds to wildtype ARNT PAS-B via two binding modes (Gagné, 2020). The surface binding of KG-655 involves sidechains of residue I364 and I458, resulting in chemical shift changes that are observed when titrated against wildtype ARNT PAS-B, but are missing from these spectra even at the highest ligand concentration (black dotted squares). Methyl groups with changes in chemical shifts (I396, L408, and M439, blue dotted squares) are all on sidechains oriented inward (inset PDB 4EQ1 (Guo et al., 2013)), to the internal cavity of the protein, suggesting the internal binding mode is retained.

References

Card, P. B., Erbel, P. J. A., and Gardner, K. H.: Structural basis of ARNT PAS-B dimerization: use of a common beta-sheet interface for hetero- and homodimerization, J. Mol. Biol., 353, 664-677, 10.1016/j.jmb.2005.08.043, 2005.

Gagné, D. A., R.; Edupuganti, U.R.; Williams, J.; Aramini, J.M.; Akasaka, K., Gardner, K.H.: Use of high pressure NMR spectroscopy to rapidly identify internal ligand-binding voids in proteins, Manuscript under review., 2020.

Guo, Y., Partch, C. L., Key, J., Card, P. B., Pashkov, V., Patel, A., Bruick, R. K., Wurdak, H., and Gardner, K. H.: Regulating the ARNT/TACC3 axis: multiple approaches to manipulating protein/protein interactions with small molecules, ACS Chem. Biol., 8, 626-635, 10.1021/cb300604u, 2013.